



**HAL**  
open science

# A split-range acquisition method for the non-targeted metabolomic profiling of human plasma with hydrophilic interaction chromatography - high-resolution mass spectrometry

Fanta Fall, Natacha Lenuzza, Elodie Lamy, Marion Brollo, Emmanuel Naline, Philippe Devillier, Etienne Thévenot, Stanislas Grassin-Delyle

## ► To cite this version:

Fanta Fall, Natacha Lenuzza, Elodie Lamy, Marion Brollo, Emmanuel Naline, et al.. A split-range acquisition method for the non-targeted metabolomic profiling of human plasma with hydrophilic interaction chromatography - high-resolution mass spectrometry. *Journal of Chromatography B - Analytical Technologies in the Biomedical and Life Sciences*, 2019, 1128, pp.121780 -. 10.1016/j.jchromb.2019.121780 . hal-03488294

**HAL Id: hal-03488294**

**<https://hal.science/hal-03488294>**

Submitted on 20 Jul 2022

**HAL** is a multi-disciplinary open access archive for the deposit and dissemination of scientific research documents, whether they are published or not. The documents may come from teaching and research institutions in France or abroad, or from public or private research centers.

L'archive ouverte pluridisciplinaire **HAL**, est destinée au dépôt et à la diffusion de documents scientifiques de niveau recherche, publiés ou non, émanant des établissements d'enseignement et de recherche français ou étrangers, des laboratoires publics ou privés.



Distributed under a Creative Commons Attribution - NonCommercial 4.0 International License

1                   **A split-range acquisition method for the non-targeted**  
2                   **metabolomic profiling of human plasma with hydrophilic**  
3                   **interaction chromatography - high-resolution mass spectrometry**

4

5 Fanta Fall,<sup>1</sup> Natacha Lenuzza,<sup>2</sup> Elodie Lamy,<sup>1</sup> Marion Brollo,<sup>3</sup> Emmanuel Naline,<sup>3,4</sup> Philippe  
6 Devillier,<sup>3,4</sup> Etienne Thévenot,<sup>2</sup> Stanislas Grassin-Delyle<sup>1,4</sup>

7

8 <sup>1</sup>INSERM U1173, plateforme de spectrométrie de masse, UFR Simone Veil - Santé,  
9 Université Versailles – Saint Quentin en Yvelines, Université Paris Saclay, Montigny le  
10 Bretonneux, France

11 <sup>2</sup>CEA, LIST, Laboratory for Data Sciences and Decision, MetaboHUB-Paris, Gif-sur-Yvette,  
12 France

13 <sup>3</sup>UPRES EA220, Université Versailles – Saint Quentin en Yvelines, Université Paris Saclay,  
14 Suresnes, France

15 <sup>4</sup>Département des maladies des voies respiratoires, Hôpital Foch, Suresnes, France

16

17

18 **Corresponding author:** Stanislas Grassin-Delyle, INSERM UMR 1173, Plateforme de  
19 spectrométrie de masse MasSpecLab, UFR Simone Veil - Santé, 2 avenue de la source de la  
20 Bièvre, 78180 Montigny le Bretonneux, France. Phone: +33.1.70.42.94.22. E-mail address:  
21 stanislas.grassin-delyle@uvsq.fr

22

23 **ABSTRACT**

24

25 Untargeted metabolomics of human plasma with mass spectrometry is of particular interest in  
26 medical research to explore pathophysiology, find disease biomarkers or for the  
27 understanding of the response to pharmacotherapy. Since analytical performances may be  
28 impacted by the laboratory environment and the acquisition method settings, the objectives of  
29 this study were to assess the role of interfering compounds and to propose an acquisition  
30 method to maximise the metabolome coverage for human plasma metabolomic analysis.  
31 Human plasma samples were processed with liquid/liquid extraction then analysed with  
32 HILIC-high resolution mass spectrometry. A method with a single  $m/z$  range was compared to  
33 four methods with different split acquisition ranges and four sets of ionization source  
34 parameters were compared. The data were analysed with the R software and on the  
35 Worklow4Metabolomics online platform.

36 The major interfering compounds were identified in blank samples where they accounted for  
37 up to 86% of the signal intensity. Splitting the acquisition range into 3  $m/z$  ranges improved  
38 the number of detected features, the number of features with proposed annotation in the  
39 Human Metabolome Database, as well as signal intensity throughout the whole  $m/z$  range.  
40 The method performing best was the one using three  $m/z$  ranges of approximatively the same  
41 extent. Ionization source parameters also strongly affected the number of detected features.  
42 Splitting the acquisition range into 3  $m/z$  ranges with optimised ionisation source parameters  
43 allows a comprehensive analysis of the human plasma metabolome with perspectives for  
44 applications to pathophysiological studies.

45

46 **KEYWORDS:** metabolomics; high-resolution mass spectrometry; hydrophilic interaction  
47 liquid chromatography; human plasma

## 48 1. INTRODUCTION

49 Metabolomics is a phenotyping approach interested in molecules located downstream (in  
50 biological terms) of those targeted by established genomics, transcriptomics and proteomics  
51 approaches. It provides novel insights into mechanisms of disease pathogenesis and is useful  
52 for the discovery of biomarkers for disease diagnosis, prognosis or for the prediction of the  
53 response to pharmacotherapy in the era of precision medicine [1, 2]. As for the above-  
54 mentioned classical “omics” technologies, untargeted approaches are best suited for the  
55 discovery of biomarkers and mass spectrometry (MS) has become the most convenient  
56 analytical platform for the sensitive and comprehensive metabolomic profiling of human  
57 tissues and fluids, especially with the expansion of high-resolution instruments. Plasma is the  
58 biofluid of choice for human studies, it is easy to collect and reflects the systemic metabolism.  
59 It contains thousands of metabolites of varying abundance, molecular weight, polarity, water  
60 solubility and ionization states which may each require specific analytical conditions to be  
61 detected. Therefore, the interest of combining hydrophilic interaction liquid chromatography  
62 (HILIC) and reverse-phase (RP) liquid chromatography to improve the coverage of plasma  
63 metabolome has already been reported [3-6]. Although the aim of the analysis is to focus only  
64 on molecules present in the plasma sample, the performance of untargeted analysis may also  
65 be impacted by interfering compounds from the laboratory environment, i.e. in the materials,  
66 reagents or in the analytical instruments as a residue from previous analytical runs. Well-  
67 described interferences are proteins, solvents, polymers, plastics and additives such as  
68 detergents or ion pairing reagents, which are known to affect MS analysis [7]. Optimal  
69 acquisition parameters should therefore both maximize the detection of compounds of interest  
70 and minimize the influence of contaminants. However, despite the widespread use of  
71 metabolomic analysis, the influence of exogenous contaminants and the optimisation of mass  
72 spectrometry parameters for the metabolomic analysis of human plasma has never been

73 investigated to date. The objectives of the present study were first to assess the main  
74 interfering compounds in a laboratory setting then to propose an analytical strategy to  
75 maximize the number of compounds detected in human plasma. HILIC was retained for  
76 chromatography since it was described to have the widest serum metabolome coverage [3].  
77

## 78 **2. MATERIALS AND METHODS**

### 79 **2.1.Reagents**

80 LC-MS-grade ammonium formate and formic acid (98%) were supplied by Sigma Aldrich  
81 (Saint Quentin Fallavier, France). LC-MS-grade methanol, acetonitrile, chloroform and water  
82 were from Fisher Scientific (Illkirch, France). Deuterated internal standards (IS) were from  
83 Bertin technologies (Montigny le Bretonneux, France) (anandamide-d<sub>4</sub>, 25-  
84 hydroxycholesterol-d<sub>6</sub>, 2-arachidonoylglycerol-d<sub>8</sub>) and LCG standards (St. Louis, MO, USA)  
85 (hydrocortisone-d<sub>4</sub>, glyburide-d<sub>3</sub>, fludrocortisone-d<sub>2</sub>, testosterone-d<sub>3</sub>, propoxyphene-d<sub>5</sub>,  
86 chlorpromazine-d<sub>3</sub> and fluoxetine-d<sub>6</sub>). Plasma was obtained from the local blood bank  
87 (Etablissement Français du Sang, Rungis, France).

88

### 89 **2.2.Sample preparation**

90 One hundred microliters of plasma were spiked with 10 µL of the mix of deuterated internal  
91 standards (anandamide-d<sub>4</sub>, 25-hydroxycholesterol-d<sub>6</sub>, 2-arachidonoylglycerol-d<sub>8</sub>,  
92 hydrocortisone-d<sub>4</sub> and glyburide-d<sub>3</sub>, 0.5 mg L<sup>-1</sup> and fludrocortisone-d<sub>2</sub>, testosterone-d<sub>3</sub>,  
93 propoxyphene-d<sub>5</sub>, chlorpromazine-d<sub>3</sub> and fluoxetine-d<sub>6</sub>, 0.05 mg L<sup>-1</sup>) then subjected to  
94 liquid/liquid extraction using 1 mL of methanol/chloroform/water (1:2:1 v/v/v) [8]. The  
95 mixture was vortexed for 30 seconds, agitated for 20 mins and centrifuged at 10000 rpm for 5  
96 mins. 200 µL of upper phase were collected and dried under vacuum. The dried extracts were  
97 reconstituted with 75 µL of ammonium formate/acetonitrile (20:80 v/v) and transferred into  
98 injection vials for analysis. Plasma samples from 3 different healthy donors were analyzed in  
99 triplicate in each experimental condition together with blank samples consisting in mobile  
100 phase only. Samples were injected in random order.

101

### 102 **2.3.Chromatographic separation**

103 Chromatography was performed with an UltiMate 3000 system (Thermo Scientific Dionex,  
104 Les Ulis, France). A SeQuant<sup>®</sup> 4.6 mm x 150 mm, 5 µm i.d. ZIC-pHILIC column (AIT  
105 France, Houilles, France) was used for chromatography [9]. Separation was performed under  
106 gradient elution using a mobile phase system consisting of ammonium formate 10 mM pH 3.8  
107 (solvent A) and acetonitrile (solvent B). Starting conditions were 95% solvent B for 3 min  
108 then reaching 8% at 25 min. This plateau was kept for 5 more minutes, then back to 95% and  
109 equilibration for 10 minutes. Flow rate was 0.3 mL min<sup>-1</sup> and oven temperature 40°C.

110

## 111 **2.4.High-resolution mass spectrometry analysis**

112 Compounds were detected with a Q-Exactive mass spectrometer (ThermoFisher) equipped  
113 with a heated electrospray ionization (HESI) source. Nitrogen (N2-45 nitrogen generator,  
114 VWR International, Fontenay sous bois, France) was employed as sheath and auxiliary gas.

115

### 116 *2.4.1. Source parameters*

117 The HESI source was set in the positive ionization mode with a capillary temperature of  
118 275°C. Unless otherwise stated, sheath and auxiliary gas flow rate were set at 40 and 25  
119 arbitrary units, respectively; S-lens RF level at 100, spray voltage at 4000 V and temperature  
120 of vaporization at 100°C.

121

### 122 *2.4.2. Acquisition parameters*

123 In the first part of the study, samples were analyzed using a single full-scan  $m/z$  range (60-  
124 900) to identify the main analytical interferences. Then, four other acquisition methods were  
125 evaluated to assess the influence of splitting the scan range at masses of the main interfering  
126 compounds. Comparison was performed between the full-scan method ( $m/z$  60-900, method  
127 M1) and different split methods (Figure 1): method M2 (3  $m/z$  ranges,  $m/z$  60-101; 105-213;

128 215-900), method M3 (3  $m/z$  ranges,  $m/z$  60-81; 85-213; 215-900), method M4 (3  $m/z$  ranges,  
129  $m/z$  60-82; 82-213; 213-900) and method M5 (3  $m/z$  ranges,  $m/z$  60-300; 300-600; 600-900).  
130 Resolution was set at 70000, AGC target at  $10^6$  and maximum IT at 256 ms. Data acquisition  
131 was performed using Chromeleon v 6.80 and Xcalibur v3.0.63 (ThermoFisher).

132

## 133 **2.5.Data analysis**

134 XCalibur RAW files were first converted to mzML and centroidized with msConvert [10],  
135 then processed using IPO [11] and XCMS (v1.50.1) [12] packages running under R. The  
136 CentWave algorithm [13] was used for automatic peak picking: ppm = 10, snthresh = 10,  
137 peakwidth = 15-70, mzdifff= 0.01 and prefilter = c(3, 5000), with the peakwidth parameter  
138 optimized with IPO. Alignment step was performed using the group.density method (bw = 5,  
139 mzwid = 0.01, minfrac = 0.5) and retcor.loess method (missing = n\_blank+1, extra = 1). The  
140 peak table obtained at this step therefore contained the total number of peaks in study  
141 samples. Then, several filters were applied to exclude non-relevant peaks (based on analytical  
142 criteria) detected by XCMS [14] (Supplementary Figure 1): first, robust peaks were defined as  
143 peaks found in  $\geq 2$  of the samples of at least one condition; then all features with a retention  
144 time outside the window 3-30 min were discarded (retention time filter) and features detected  
145 in biological samples with a mean intensity less than 2-fold the intensity observed in blank  
146 samples, or features detected in blank samples only were also filtered out (signal filter). This  
147 group therefore constitutes the “robust, relevant peaks” group. The peak picking score (PPS)  
148 obtained with the IPO algorithm was used to assess the quality of the peak list obtained which  
149 each method. PPS was defined as the ratio of reliable peaks (RP) (which are peaks part of an  
150 isotopologue consisting of  $^{13}\text{C}$  isotope peaks) weighted by the exponential factor 2, to the  
151 total number of peaks ( $((\text{number of reliable peaks})^2 / (\text{total number of peaks}))$ ). Therefore, if the



152 RP value and the total number of relevant peaks increase by the same amount, the PPS  
153 increases. All these filtering steps and peak definitions are shown in Supplementary Figure 1.  
154

### 155 3. RESULTS AND DISCUSSION

#### 156 3.1.Evaluation of interferences

157 Interferences originating from the laboratory environment and unrelated to plasma samples  
158 were assessed by the examination of ions present in blank samples (Figure 2). Three profiles  
159 were found for the most abundant interfering ions: intermittent interferences occurring at a  
160 specific retention time ( $m/z$  102.1274 and 104.1066); interferences present during a  
161 significant part of the run ( $m/z$  167.0123 and 214.0892) and interferences present during the  
162 whole run ( $m/z$  83.0602). The signal intensity for those interfering compounds was between  
163  $10^7$  and  $4 \cdot 10^9$ , which accounted up to a maximum of 85.7% of the total signal. The major  
164 interferences were identified as being acetonitrile ( $m/z$  83.0602), triethylamine ( $m/z$  102.1274)  
165 and n-butyl benzenesulfonamide ( $m/z$  214.0892). Acetonitrile originates from mobile phase,  
166 triethylamine was previously used on the same instrument and is well-described to have a  
167 persistent memory effect in LC-MS [15], and n-butyl benzenesulfonamide is a widespread  
168 plasticizer [7]. Considering the signal intensity observed for these molecules, the C-trap  
169 should be filled faster with interferences, which in turn should decrease the sensitivity for  
170 compounds of interest. Therefore, the effect of splitting the acquisition  $m/z$  range was  
171 examined to avoid the acquisition of the main interfering compounds and possibly enhance  
172 the detection of metabolites.

173

#### 174 3.2.Effect of excluding interfering compounds from acquisition

175 The  $m/z$  of the most intense intermittent interferences ( $m/z$  102.1274 and 104.1066) as well as  
176 from n-butyl benzenesulfonamide ( $m/z$  214.0892) were first excluded from the acquisition  
177 method (Figure 1; M2 acquisition method). The comparison of the triplicate analysis of  
178 plasma samples with the original M1 method and this modified M2 method resulted in the  
179 increase of the mean total number of peaks from 5,366 to 15,304 peaks, with a corresponding

180 increase of robust, relevant peaks from 2,892 to 8,340 peaks (Table 1). 368 peaks were  
181 specific of the M1 method; 2,210 of the M2 method while 3,086 were common to both  
182 methods (Supplementary Table 1). The peaks specific to the M2 method were equally  
183 distributed over all the  $m/z$  range and mostly detected in the first 10 min or between 15-20  
184 min of the analytical run (Figure 3A).  
185 Then, the  $m/z$  ranges of the interference detected during the whole run (acetonitrile,  $m/z$   
186 83.0602) as well as from n-butyl benzenesulfonamide ( $m/z$  214.0892) were excluded (Figure  
187 1, method M3). For this M3 method, the total number of peaks was 14,848, corresponding to  
188 8,203 robust, relevant peaks. 2,019 peaks were specific of the M3 method (compared to M1;  
189 Supplementary Table 1). As for method M2, these peaks were equally distributed over the  $m/z$   
190 range and mostly detected in the first 10 min or between 15-20 min of the analytical run  
191 (Figure 3B). Altogether, these results suggest that excluding interfering  $m/z$  from the  
192 acquisition allows a better detection of the sample compounds all over the  $m/z$  -and time-  
193 ranges.

194

### 195 **3.3.Effect of $m/z$ range splitting**

196 Since splitting the  $m/z$  range systematically increased the number of peaks detected, we  
197 addressed whether this observation was due to the exclusion of interferences or if it was the  
198 consequence of splitting the acquisition method into several  $m/z$  ranges. The method M2 was  
199 therefore compared to method M4 where the acquisition range was split into three continuous  
200 ranges, without any gap between each range (Figure 1). As shown in Table 1, both methods  
201 allowed the detection of an equivalent number of total and robust, relevant peaks and 5,441  
202 features were common to both methods (Supplementary Table 1). This suggests that splitting  
203 the scan range is more useful for increasing the number of detected compounds than  
204 excluding specific interferences.

205

### 206 **3.4.Effect of $m/z$ range size**

207 Finally, in order to fully assess the impact of  $m/z$  range splitting, a new M5 method was  
208 designed, where the  $m/z$  interval of each of the 3 split ranges was between 240-300 units  
209 (Figure 1). Optimizing the size of  $m/z$  ranges increased the number of robust, relevant peaks  
210 from 8,272 to 11,005 (33% increase in comparison to the M4 method), as shown in Table 1.  
211 4,781 peaks were common to both methods whereas 1,764 peaks were specific of the M5  
212 method. The gain in the number of peaks detected is mainly in the  $m/z$  range from 300 to 900  
213 (Supplementary Table 1 and Supplementary Figure 2). With this latest M5 method, the PPS  
214 score was the highest obtained among the 5 methods. The mass spectrometric fundamentals  
215 explaining this phenomenon for Q-Exactive instruments are related to the value of the voltage  
216 applied to the focusing lenses (RF) of the C-trap. This voltage is automatically adapted to the  
217 smallest mass value of the scan by the instrument and cannot be modified. For example, for a  
218 scan of 60 to 900  $m/z$  it is set to allow optimal extraction of small mass ions, and therefore the  
219 extraction of high mass ions will not be optimal. By dividing the same mass range into 3  
220 segments (60-300, 300-600 and 600-900  $m/z$ ), and thus into 3 consecutive scans, an RF value  
221 is applied for each segment and depends on the smallest mass in the segment. A first value is  
222 therefore optimized for masses close to 60, a second for masses close to 300 and a third for  
223 masses close to 600. In addition, for scans from 300 to 600 and from 600 to 900  $m/z$ , the  
224 quadrupole filters all masses below 300 and 600 and therefore decreases the background noise  
225 generated by the mobile phase (or other contaminants), which allows the detection of more  
226 peaks of interest. Thus, the performance of using several consecutive scans on complementary  
227 mass ranges for methods intended to cover large mass ranges is better, because the value of  
228 the RF applied to the C-trap will be optimized for each scan and will allow a better extraction  
229 of the ions from each scan.

230 Splitting into 2 or 3  $m/z$  ranges was also compared. With a method consisting in 2  $m/z$  ranges  
231 (60-200 and 200-900), the number of relevant, robust peaks was 5,854, which is about 3-fold  
232 lower than with the 3-scan range method.

233

### 234 **3.5. Consequences on metabolite annotation**

235 Although detecting a higher number of robust, reliable peaks demonstrates increased  
236 sensitivity, understanding pathophysiological mechanisms with metabolomic analysis makes  
237 it mandatory to annotate (i.e. identify) the compounds of interest. Therefore, the number of  
238 annotated compounds after HMDB database query was compared between the initial M1 and  
239 the final M5 methods. For the M1 method, compound identification was proposed for 1,633  
240 of the relevant, robust peaks, raising to 4,397 for the M5 method *i.e.* a 169% increase in the  
241 number of peaks with proposed annotation.

242

### 243 **3.6. Consequences on signal intensity for metabolites or deuterated standards**

244 Finally, although splitting the  $m/z$  range obviously increases the number of detected features,  
245 the impact of splitting on the signal intensity of known and unknown compounds was  
246 assessed. For deuterated internal standards, mean peak area of triplicate analysis of 3 plasma  
247 samples with the M5 method was  $126 \pm 52\%$  [49-275] of the mean peak area observed with  
248 the M1 method. When comparing the signal intensity of features detected with the initial M1  
249 and final M5 method, a mean 1.6-fold increase in intensity was observed, with 25<sup>th</sup> and 75<sup>th</sup>  
250 percentiles at 0.95 and 1.85, respectively (Figure 4). This increase occurred for all 3  $m/z$   
251 ranges and was even greater for the highest  $m/z$ , whereas splitting into 2  $m/z$  ranges may  
252 induce a loss of signal in the low  $m/z$  range [16].

253

### 254 **3.7. Ionization source parameters**

255 The parameters of the ESI strongly influence the number of detected features, as shown with  
256 the metabolomic analysis of plant samples [17], and should therefore be optimized for each  
257 experimental setting. To assess whether compound detection could be further improved in  
258 human plasma with optimizing ionization source parameters, four sets of parameters were  
259 compared with low, medium, high or intermediate values for S-Lens RF level, spray voltage,  
260 sheath and auxiliary gas flow rate and temperature of vaporization (Table 2). Results are  
261 shown in Table 3. The intermediate set of parameters provided the highest number of robust,  
262 relevant peaks and highest PPS score.  
263

## 264 CONCLUSIONS

265 Scientists employing high-resolution instruments for untargeted mass spectrometry analysis,  
266 such as metabolomic studies, face new challenges with respect to the simultaneous recording  
267 of a huge number of features in a given  $m/z$  range, which may be either background noise or  
268 compounds of interest. Metabolites are considered to be molecules with a molecular weight  
269 less than 1,000 Da, which implies to cover a mass range between about 50 and 1,000 Da to  
270 ensure the widest coverage. In the vast majority of methods described to date, a single  
271 acquisition range as well as generic ionization source parameters were used. Although a  
272 strategy for splitting the acquisition range into a low and high  $m/z$  ranges was previously  
273 investigated for the analysis of renal cell metabolome with reverse-phase chromatography  
274 [16], no investigation with an interference-driven splitting strategy was reported to date for  
275 the analysis of human plasma. The results of the present study show the interest of splitting  
276 the  $m/z$  acquisition range into 3 segments for the metabolomic analysis of human plasma with  
277 hydrophilic interaction liquid chromatography coupled to high-resolution mass spectrometry.  
278 Since acquisition range splitting outperforms excluding the acquisition of the main  
279 interferences, such strategy may be universally applied, regardless of the contaminants that  
280 may be present in each laboratory environment. The performance gain affects both the  
281 number of compounds detected and also the number of molecules for which an annotation can  
282 be proposed by querying the databases, which is the final goal of the metabolomic analysis. In  
283 addition, sensitivity was also improved throughout the entire  $m/z$  range whereas different  
284 splitting strategies may induce a loss of signal [16]. In combination with the optimization of  
285 the ionization source parameters, the proposed method therefore allows a more  
286 comprehensive analysis of the human plasma metabolome which may be applied to  
287 pathophysiological studies.

288

289 **TABLES**290 **Table 1:** Number of peaks in each method before and after filtering.

291

<b>Method</b>	<b>Total peaks in blank sample (n)</b>	<b>Total peaks in study samples (mean [min-max])</b>	<b>Robust peaks (mean [min-max])</b>	<b>RT-filtered robust peaks (mean [min-max])</b>	<b>Robust, relevant peaks (signal- and RT-filtered robust peaks) (mean [min-max])</b>	<b>PPS</b>
M1	1,879	5,366 [5,060-5,669]	4,689 [4,528-4,982]	3,970 [3,758-4,292]	2,892 [2,615-3,315]	3,283
M2	6,876	15,304 [14,557-15,762]	12,858 [11,832-13,751]	10,612 [9,745-11,362]	8,340 [7,472-9,128]	6,707
M3	6,960	14,848 [13,932-15,445]	12,515 [11,620-13,132]	10,357 [9,535-10,920]	8,203 [7,443-8,827]	6,874
M4	7,983	14,721 [14,130-15,197]	12,473 [11,531-12,963]	10,287 [9,386-10,769]	8,272 [7,387-8,851]	6,847
M5	9,068	18,697 [17,695-19,296]	16,076 [15,098-15,592]	12,874 [11,933-13,377]	11,005 [10,146-11,542]	8,162

292

293 RT: retention time; PPS: peak picking score (the highest the better)

294



295 **Table 2:** Sets of parameters of the ionization source

296

---

<b>Parameter</b>	<b>Low</b>	<b>Medium</b>	<b>Intermediate</b>	<b>High</b>
S-lens RF level	50	75	100	100
Spray voltage	1,500	3,000	4,000	5,000
Sheath gas flow rate	10	35	40	60
Aux gas flow rate	5	15	25	30
Temperature of vaporization	100	200	100	300

---

297

298

299 **Table 3:** Effect of ionization source parameters on peak detection

300

<b>Method</b>	<b>Total peaks in blank sample (n)</b>	<b>Total peaks in study samples (n)</b>	<b>Robust peaks (n)</b>	<b>RT-filtered robust peaks (n)</b>	<b>Robust, relevant peaks (signal- and RT-filtered robust peaks) (n)</b>	<b>PPS</b>
Low	2,938	7,211	5,836	5,199	3,220	2,629
Medium	11,807	20,259	12,755	9,184	5,272	3,576
Intermediate	7,010	16,889	13,625	10,314	6,588	4,153
High	8,376	19,187	14,510	11,026	5,895	2,678

301

302 RT: retention time; PPS: peak picking score (the highest the better)

303

304 **FIGURE LEGENDS**

305

306 **Figure 1: Schematic overview of the different acquisition methods.**  $m/z$  splitting ranges  
307 are depicted for each method. SR = scan range.

308

309 **Figure 2: Extracted ion chromatograms of interfering compounds.** Each colour  
310 corresponds to a plasma sample from a different donor.

311

312 **Figure 3: Comparison of features between the M1 and M2 (A) and M1 and M3 (B)**  
313 **acquisition methods.**  $m/z$  and retention time are represented for each feature (after retention  
314 time and signal filtering), for features specific to each method and features common to both  
315 methods. The green, blue and red dots represent the 3 plasma samples which were analysed in  
316 triplicates.

317

318 **Figure 4: Intensity ratio for features common to the M5 and M1 methods.** The M5/M1  
319 ratio (log scale) are shown as a function of  $m/z$ . The horizontal dashed gray line represents the  
320 identity line, the horizontal black line represents the mean, vertical grey lines represent the  
321  $m/z$  ranges of the M5 method.

322

323 **REFERENCES**

- 324 [1] P. Devillier, H. Salvator, E. Naline, L.J. Couderc, S. Grassin-Delyle, *Metabolomics in the*  
325 *Diagnosis and Pharmacotherapy of Lung Diseases*, *Curr Pharm Des*, 23 (2017) 2050-2059.
- 326 [2] L. Guo, M.V. Milburn, J.A. Ryals, S.C. Lonergan, M.W. Mitchell, J.E. Wulff, D.C.  
327 Alexander, A.M. Evans, B. Bridgewater, L. Miller, M.L. Gonzalez-Garay, C.T. Caskey, *Plasma*  
328 *metabolomic profiles enhance precision medicine for volunteers of normal health*, *Proc Natl*  
329 *Acad Sci U S A*, 112 (2015) E4901-4910.
- 330 [3] S. Boudah, M.F. Olivier, S. Aros-Calt, L. Oliveira, F. Fenaille, J.C. Tabet, C. Junot,  
331 *Annotation of the human serum metabolome by coupling three liquid chromatography methods*  
332 *to high-resolution mass spectrometry*, *J Chromatogr B Analyt Technol Biomed Life Sci*, 966  
333 (2014) 34-47.
- 334 [4] K. Contrepolis, L. Jiang, M. Snyder, *Optimized Analytical Procedures for the Untargeted*  
335 *Metabolomic Profiling of Human Urine and Plasma by Combining Hydrophilic Interaction*  
336 *(HILIC) and Reverse-Phase Liquid Chromatography (RPLC)-Mass Spectrometry*, *Mol Cell*  
337 *Proteomics*, 14 (2015) 1684-1695.
- 338 [5] D.Q. Tang, L. Zou, X.X. Yin, C.N. Ong, *HILIC-MS for metabolomics: An attractive and*  
339 *complementary approach to RPLC-MS*, *Mass Spectrom Rev*, 35 (2016) 574-600.
- 340 [6] C. Virgiliou, H.G. Gika, G.A. Theodoridis, *HILIC-MS/MS Multi-Targeted Method for*  
341 *Metabolomics Applications*, *Methods Mol Biol*, 1738 (2018) 65-81.
- 342 [7] B.O. Keller, J. Sui, A.B. Young, R.M. Whittall, *Interferences and contaminants encountered*  
343 *in modern mass spectrometry*, *Anal Chim Acta*, 627 (2008) 71-81.
- 344 [8] E.G. Bligh, W.J. Dyer, *A rapid method of total lipid extraction and purification*, *Can J*  
345 *Biochem Physiol*, 37 (1959) 911-917.
- 346 [9] R. Zhang, D.G. Watson, L. Wang, G.D. Westrop, G.H. Coombs, T. Zhang, *Evaluation of*  
347 *mobile phase characteristics on three zwitterionic columns in hydrophilic interaction liquid*

348 chromatography mode for liquid chromatography-high resolution mass spectrometry based  
349 untargeted metabolite profiling of Leishmania parasites, *J Chromatogr A*, 1362 (2014) 168-  
350 179.

351 [10] D. Kessner, M. Chambers, R. Burke, D. Agus, P. Mallick, ProteoWizard: open source  
352 software for rapid proteomics tools development, *Bioinformatics*, 24 (2008) 2534-2536.

353 [11] G. Libiseller, M. Dvorzak, U. Kleb, E. Gander, T. Eisenberg, F. Madeo, S. Neumann, G.  
354 Trausinger, F. Sinner, T. Pieber, C. Magnes, IPO: a tool for automated optimization of XCMS  
355 parameters, *BMC Bioinformatics*, 16 (2015) 118.

356 [12] C.A. Smith, E.J. Want, G. O'Maille, R. Abagyan, G. Siuzdak, XCMS: processing mass  
357 spectrometry data for metabolite profiling using nonlinear peak alignment, matching, and  
358 identification, *Analytical chemistry*, 78 (2006) 779-787.

359 [13] R. Tautenhahn, C. Bottcher, S. Neumann, Highly sensitive feature detection for high  
360 resolution LC/MS, *BMC Bioinformatics*, 9 (2008) 504.

361 [14] O.D. Myers, S.J. Sumner, S. Li, S. Barnes, X. Du, One Step Forward for Reducing False  
362 Positive and False Negative Compound Identifications from Mass Spectrometry Metabolomics  
363 Data: New Algorithms for Constructing Extracted Ion Chromatograms and Detecting  
364 Chromatographic Peaks, *Analytical chemistry*, 89 (2017) 8696-8703.

365 [15] H. Rutters, T. Mohring, J. Rullkotter, J. Griep-Raming, J.O. Metzger, The persistent  
366 memory effect of triethylamine in the analysis of phospholipids by liquid chromatography/mass  
367 spectrometry, *Rapid Commun Mass Spectrom*, 14 (2000) 122-123.

368 [16] C. Ranninger, L.E. Schmidt, M. Rurik, A. Limonciel, P. Jennings, O. Kohlbacher, C.G.  
369 Huber, Improving global feature detectabilities through scan range splitting for untargeted  
370 metabolomics by high-performance liquid chromatography-Orbitrap mass spectrometry, *Anal*  
371 *Chim Acta*, 930 (2016) 13-22.

372 [17] F. Tugizimana, P.A. Steenkamp, L.A. Pieter, I.A. Dubery, Mass spectrometry in untargeted  
373 liquid chromatography/mass spectrometry metabolomics: Electrospray ionisation parameters  
374 and global coverage of the metabolome, Rapid Commun Mass Spectrom, 32 (2018) 121-132.

375

376 **COMPETING INTERESTS STATEMENT**

377 The authors have nothing to declare.

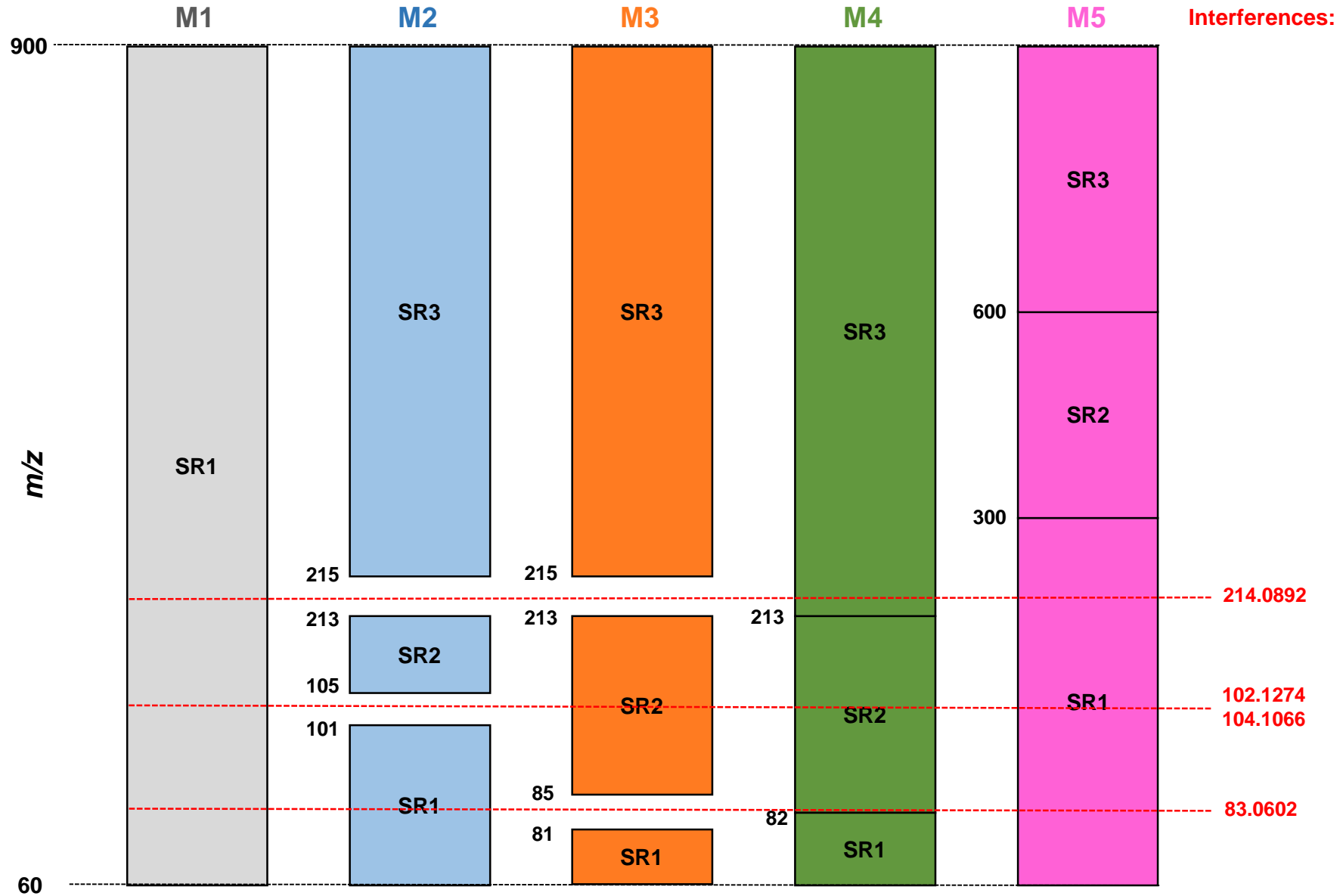
378

379 **FUNDING SOURCES**

380 This work was supported by the French Ministry of Higher Education and Research (PhD

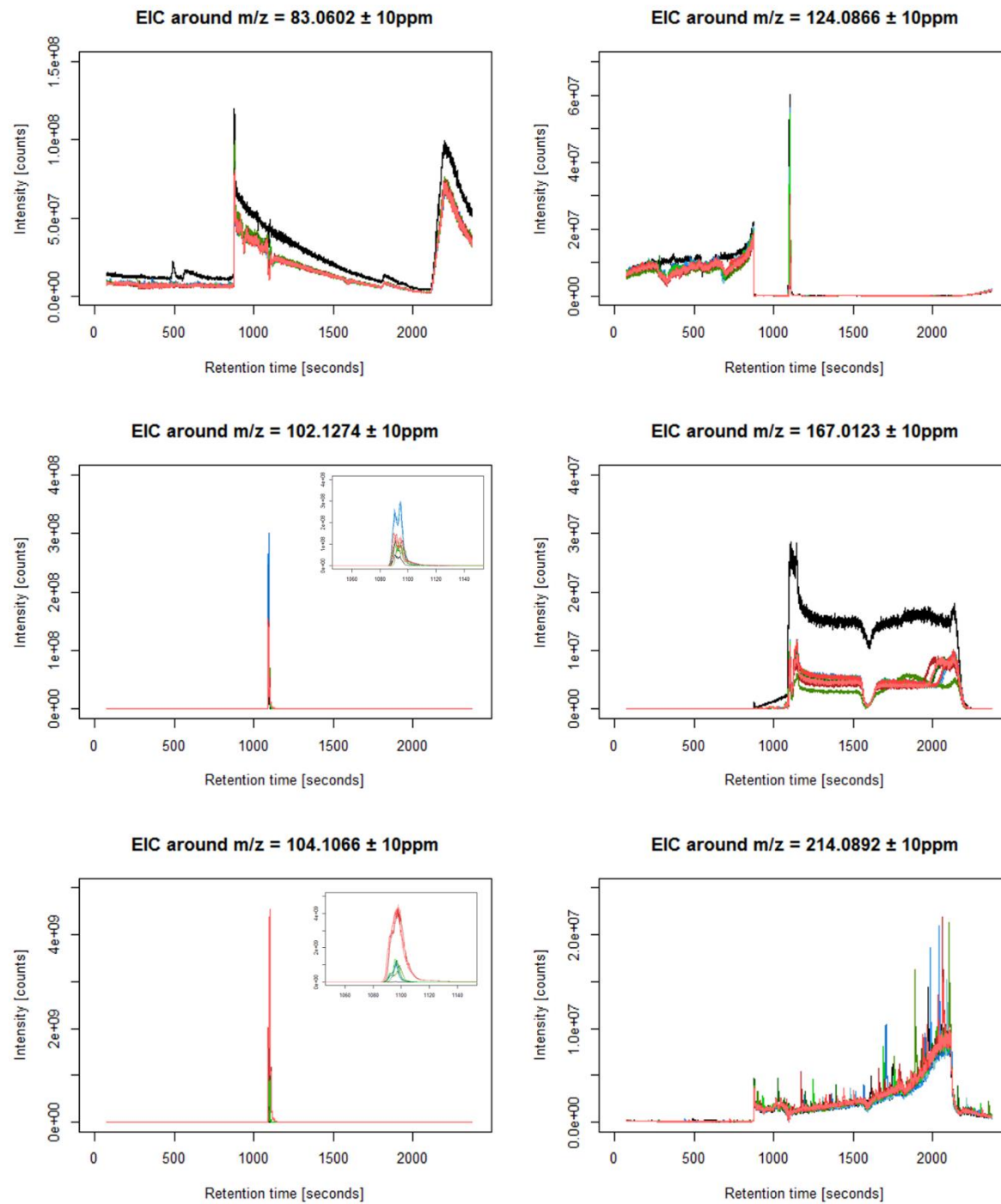
381 grant, Fanta Fall).

Figure 1





**Figure 2**



**Figure 3**

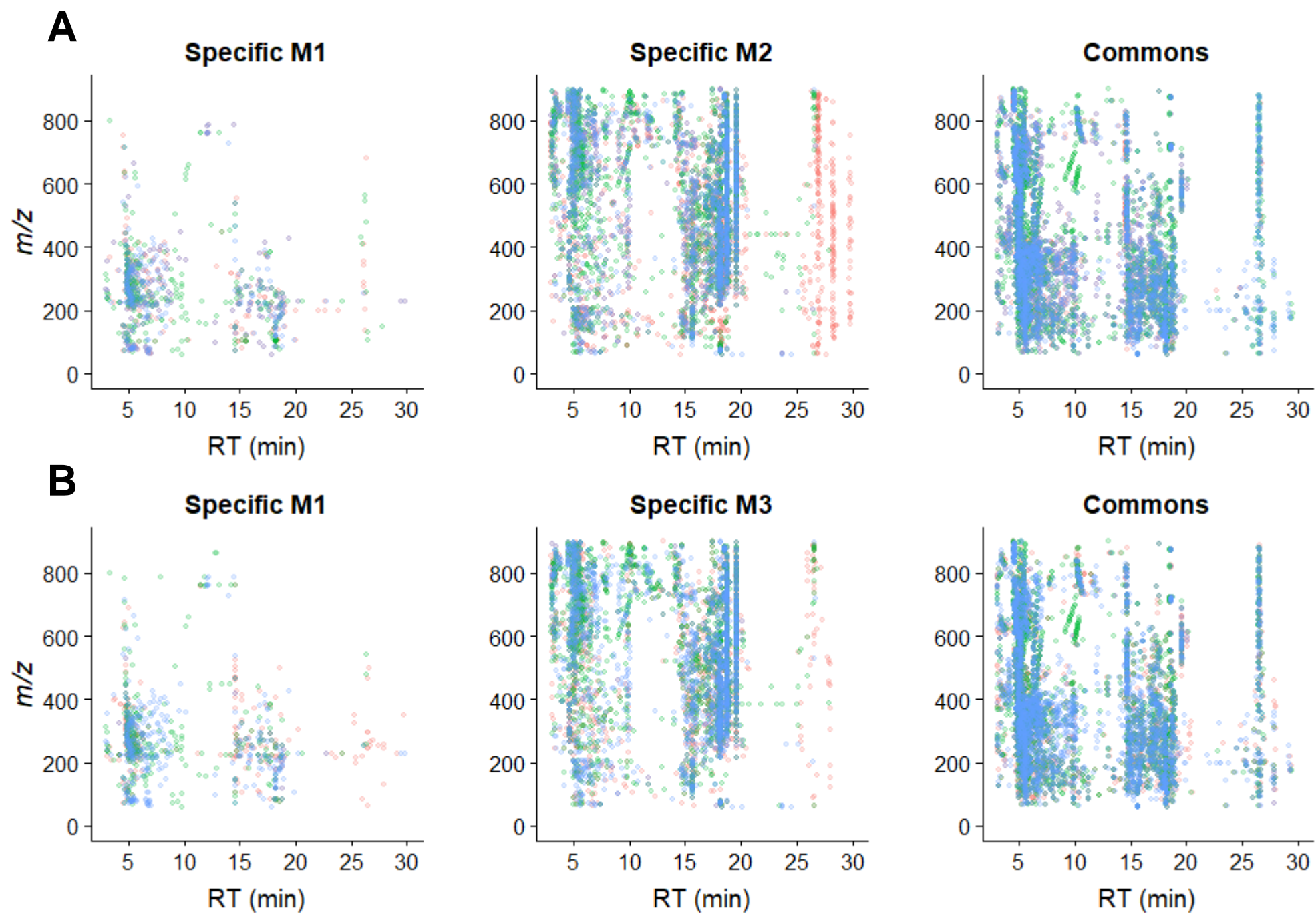


Figure 4

